



# Novel features for capturing temporal variations of rhythmic limb movement to distinguish convulsive epileptic and psychogenic nonepileptic seizures

Shitanshu Kusmakar<sup>1</sup> | Chandan Karmakar<sup>1,2</sup> | Bernard Yan<sup>3</sup> |  
Ramanathan Muthuganapathy<sup>4</sup> | Patrick Kwan<sup>3,5,6</sup> | Terence J O'Brien<sup>3,5,6</sup> |  
Marimuthu Swami Palaniswami<sup>1</sup>

<sup>1</sup>Department of Electrical and Electronic Engineering, The University of Melbourne, Melbourne, Victoria, Australia

<sup>2</sup>School of Information Technology, Deakin University, Geelong, Victoria, Australia

<sup>3</sup>Melbourne Brain Centre, Department of Medicine, The Royal Melbourne Hospital, University of Melbourne, Melbourne, Victoria, Australia

<sup>4</sup>Department of Engineering Design, Indian Institute of Technology Madras, Chennai, India

<sup>5</sup>Department of Neurosciences and Neurology, The Central Clinical School, Alfred Hospital, Monash University, Melbourne, Victoria, Australia

<sup>6</sup>Department of Medicine and Neurology, The Royal Melbourne Hospital, The University of Melbourne, Melbourne, Victoria, Australia

## Correspondence

Chandan Karmakar, School of Information Technology, Deakin University, Geelong, VIC, Australia.  
Email: karmakar@deakin.edu.au

## Summary

**Objective:** To investigate the characteristics of motor manifestation during convulsive epileptic and psychogenic nonepileptic seizures (PNES), captured using a wrist-worn accelerometer (ACM) device. The main goal was to find quantitative ACM features that can differentiate between convulsive epileptic and convulsive PNES.

**Methods:** In this study, motor data were recorded using wrist-worn ACM-based devices. A total of 83 clinical events were recorded: 39 generalized tonic-clonic seizures (GTCS) from 12 patients with epilepsy, and 44 convulsive PNES from 7 patients (one patient had both GTCS and PNES). The temporal variations in the ACM traces corresponding to 39 GTCS and 44 convulsive PNES events were extracted using Poincaré maps. Two new indices—tonic index (TI) and dispersion decay index (DDI)—were used to quantify the Poincaré-derived temporal variations for every GTCS and convulsive PNES event.

**Results:** The TI and DDI of Poincaré-derived temporal variations for GTCS events were higher in comparison to convulsive PNES events ( $P < 0.001$ ). The onset and the subsiding patterns captured by TI and DDI differentiated between epileptic and convulsive nonepileptic seizures. An automated classifier built using TI and DDI of Poincaré-derived temporal variations could correctly differentiate 42 (sensitivity: 95.45%) of 44 convulsive PNES events and 37 (specificity: 94.87%) of 39 GTCS events. A blinded review of the Poincaré-derived temporal variations in GTCS and convulsive PNES by epileptologists differentiated 26 (sensitivity: 70.27%) of 44 PNES events and 33 (specificity: 86.84%) of 39 GTCS events correctly.

**Significance:** In addition to quantifying the motor manifestation mechanism of GTCS and convulsive PNES, the proposed approach also has diagnostic significance. The new ACM features incorporate clinical characteristics of GTCS and PNES, thus providing an accurate, low-cost, and practical alternative to differential diagnosis of PNES.

## KEYWORDS

accelerometer, accelerometer features, convulsive seizures, differential diagnosis, psychogenic nonepileptic seizures

## 1 | INTRODUCTION

Psychogenic nonepileptic seizures (PNES) are sporadic paroxysmal events that are accompanied by an apparent change in state of consciousness or behavior without any epileptiform activity in the brain, where the etiology is believed to be primarily psychological.<sup>1</sup> There is no accepted pathophysiologically defined mechanism for PNES; however, PNES events are found to have an association with sporadic attacks resulting from autonomic malfunction linked to major psychosocial distress.<sup>2</sup> PNES are involuntary, and can be associated with random movements and sensory and mental manifestations resembling generalized epileptic tonic-clonic seizures (GTCS),<sup>3</sup> and are often misdiagnosed as such.<sup>4</sup>

Although a number of clinical features such as postictal serum prolactin, postictal confusion, eye-widening, and seizure duration have been proposed to assist with diagnostically distinguishing PNES from epileptic GTCS, the sensitivity and specificity of these features is insufficient to establish a definitive diagnosis in many cases.<sup>5,6</sup> Moreover, patients with PNES are often diagnosed with concurrent epileptic seizures, which indicates that outpatient diagnosis of PNES is difficult.<sup>7,8</sup> Mismanagement and delayed diagnosis of PNES increase the risk of morbidity and mortality due to intubation from prolonged seizures.<sup>9,10</sup>

Definitive diagnosis of PNES currently requires long-term video-electroencephalography monitoring (VEM). However, VEM is a highly resource-intensive procedure incurring significant health care cost.<sup>11</sup> In addition, VEM can be susceptible to artifacts on electroencephalography (EEG) recording that can render the study nondiagnostic.<sup>7</sup> Despite the limitations, VEM remains the gold standard and a cost-effective approach for diagnosing PNES, as individuals with timely intervention and correct diagnosis of PNES are shown to have a better treatment outcome.<sup>12</sup> A mean delay of 5.2 years was reported until the correct diagnosis of PNES,<sup>1</sup> indicating the shortcomings and unsatisfactory nature of current diagnostic procedures.

Accelerometers (ACMs) have been shown to be an effective tool for detection of convulsive seizures especially, GTCS.<sup>13</sup> In our previous work,<sup>14</sup> we showed that ACMs can be used reliably for the detection of convulsive PNES events. However, differentiation of convulsive PNES and GTCS requires identification of unique features that can distinguish epileptic and nonepileptic motor activity. Previously, approaches based on time-frequency mapping of the rhythmic motor activity have been employed to differentiate GTCS from convulsive PNES.<sup>15,16</sup> The classical frequency- and time-frequency-based analyses are suitable for capturing variability, the existence of periodicity, and the frequency footprint of a time-varying signal; however,

### Key Points

- An alternate approach for differentiation of GTCS and PNES is developed using a wrist-worn ACM-based device
- Two novel indices—tonic index (TI) and dispersion decay index (DDI)—that incorporate the motor symptomatology of GTCS and PNES are proposed for differentiation of GTCS and convulsive PNES
- A unimodal automated classifier based on the new ACM features correctly differentiated 42 of 44 PNES (sensitivity: 95.45%) and 37 of 39 GTCS events (specificity: 94.87%)
- An ACM-based approach that has the potential for use as a diagnostic tool to assist epileptologists in differential diagnosis of convulsive PNES

to discover complex patterns such as quasi-periodic or chaotic motion, more sophisticated signal-processing techniques are required.<sup>17</sup> Poincaré map is a technique to capture complex patterns in time-varying signals.<sup>18</sup> It has been used extensively in the analysis of cardiac signals and is central to the field of heart-rate variability (HRV) analysis.<sup>19,20</sup> In addition, it can describe nonlinear dynamics of short-length signals.<sup>14</sup> Therefore, we hypothesize that the use of Poincaré maps will provide better insight about the motor manifestation characteristics of different seizure events (GTCS and PNES).

In this study, we propose new quantitative ACM features based on Poincaré-derived temporal variations in rhythmic limb movement during seizures. To our best knowledge, no study on quantification of temporal dynamics of limb movements during GTCS and convulsive PNES has been published. This study investigates the following: (a) quantitative ACM features that can differentiate GTCS and convulsive PNES, and (b) the relevance and clinical utility of a wearable ACM-based device in the differential diagnosis of convulsive PNES.

## 2 | METHODS

### 2.1 | Participants and data acquisition

In a study from 2012-2015, 79 patients undergoing VEM at the comprehensive epilepsy unit of the Royal Melbourne Hospital were recruited to the study. Patients were assessed based on the history and description of the seizures. Patients were included in the study, if they had a history of

events that mimic generalized seizures or events characterized by the presence of bilateral convulsions. Patients having intracranial monitoring or with a psychiatric disorder such that it prevents informed consent were excluded. The study was performed in accordance with the Declaration of Helsinki and was approved by the Melbourne Health Human Research Ethics Committee (HREC Project 300:259). The patients were recruited for the complete duration of VEM, which lasted at least 3 days. A wireless device with a built-in microelectromechanical system (MEMS)<sup>21</sup> ACM sensor was strapped on the wrists of the recruited patients. The data packets were sampled at a rate of 50 Hz. Movement data recorded in 3 axes with a time stamp were saved on the flash memory of the device and were later extracted for offline processing.

## 2.2 | Diagnosis of PNES vs GTCS

The diagnosis of PNES or epileptic GTCS for all recorded convulsive events was determined at a consensus meeting of 2-6 epileptologists, where a decision was made based on the clinical history, neuropsychiatric evaluation, neuroimaging studies, video-EEG, and observed seizure semiology as reported previously.<sup>1</sup> A convulsive movement was defined as simultaneous clonic or other rhythmic motor manifestation of limb(s) that lasted at least 10 seconds. Low-amplitude tremors, intermittent jerking (eg, behavioral sleep movements), and events with only mild to moderate movements were classified as nonconvulsive. This consensus classification of the seizures by epileptologists was considered as the “gold standard.” This classification was made blinded to the ACM traces.

## 2.3 | Extraction of temporal variations in limb movement patterns

Time-stamped ACM traces corresponding to seizure events were used to extract the resultant ACM signal  $r$  ( $r = \sqrt{a_x^2 + a_y^2 + a_z^2}$ ). The resultant signal was then filtered to remove the effect of static gravity and frequencies above 25 Hz. The cutoff frequency is chosen empirically, based on the analysis of rhythmic artifacts as seen on EEG. The temporal variations are then extracted from the resultant ACM signal.

The Poincaré map is a geometric representation of the time-series data, obtained by plotting each sequence in a series against the following interval.<sup>18–20</sup> It can be used to extract rhythmic and chaotic patterns as well as temporal variations of time-series data.<sup>18</sup> A Poincaré map can be quantified using standard descriptors like  $SD1$  and  $SD2$  (Equations 1 and 2).  $SD1$  captures the short-term variability

or high-frequency changes in a time-varying signal. By contrast,  $SD2$  captures long-term variations or low-frequency changes.

$$SD1^2 = \frac{1}{2} \text{Var}(r(n) - r(n+1)) \quad (1)$$

$$SD2^2 = \frac{1}{2} \text{Var}(r(n) + r(n+1) - 2\bar{r}) \quad (2)$$

where  $\text{Var}$  is the variance,  $r(n)$  denotes the resultant ACM time series,  $n \in [1 \dots N]$ ,  $r(n+1)$  represents the sequence at  $lag = 1$ , and  $\bar{r} = E[r(n)]$ . For a discrete time signal,  $lag = 1$  represents a time delay of  $1/F_s$  (s), where  $F_s$  is the sampling frequency.

In addition, multiple parameters can be extracted from a Poincaré map. Parameters like ratio ( $\frac{SD1}{SD2}$ ) and area ( $4 * \pi * SD1 * SD2$ ) obtained using the standard Poincaré descriptors capture the nonlinear dynamics of a nonstationary time sequence.<sup>19</sup> The Poincaré-derived temporal variations can be estimated by analyzing the progression of different Poincaré descriptors over the course of an event. Because events can have varied durations, the temporal progression of the Poincaré descriptors can only be compared across events if they have a uniform duration on the time axis. Therefore, all the events were resampled using cubic splines to a uniform length of 60 seconds. The event resampling does not alter the frequency content of the signal, and the temporal patterns in the ACM signal are restored.

The resultant ACM signal corresponding to the resampled event was analyzed in time epochs of 2.56 seconds with 50% overlap resulting in a total of 45 epochs (Figure 1A,B). Poincaré maps were obtained for every epoch, resulting in a graphical representation of every sequence as a function of the previous one (Figure 1C,D). Descriptors capturing both linear ( $SD1$  and  $SD2$ ) and nonlinear dynamics (ratio and area) were then computed from each Poincaré map (Figure 1E-H).

## 2.4 | Protocol for analysis of temporal variations

Events with a uniform length of 60 seconds were segmented into quartiles (Figure 1I). This allowed us to study the temporal variability in Poincaré descriptors across the different phases (onset, transition, and subsiding) of an event.

## 2.5 | Quantification of temporal variability

To quantify the tonic phase in an event we introduce a new parameter in this work, which is termed as tonic index (TI) of an event. Whereas, to capture the subsiding nature

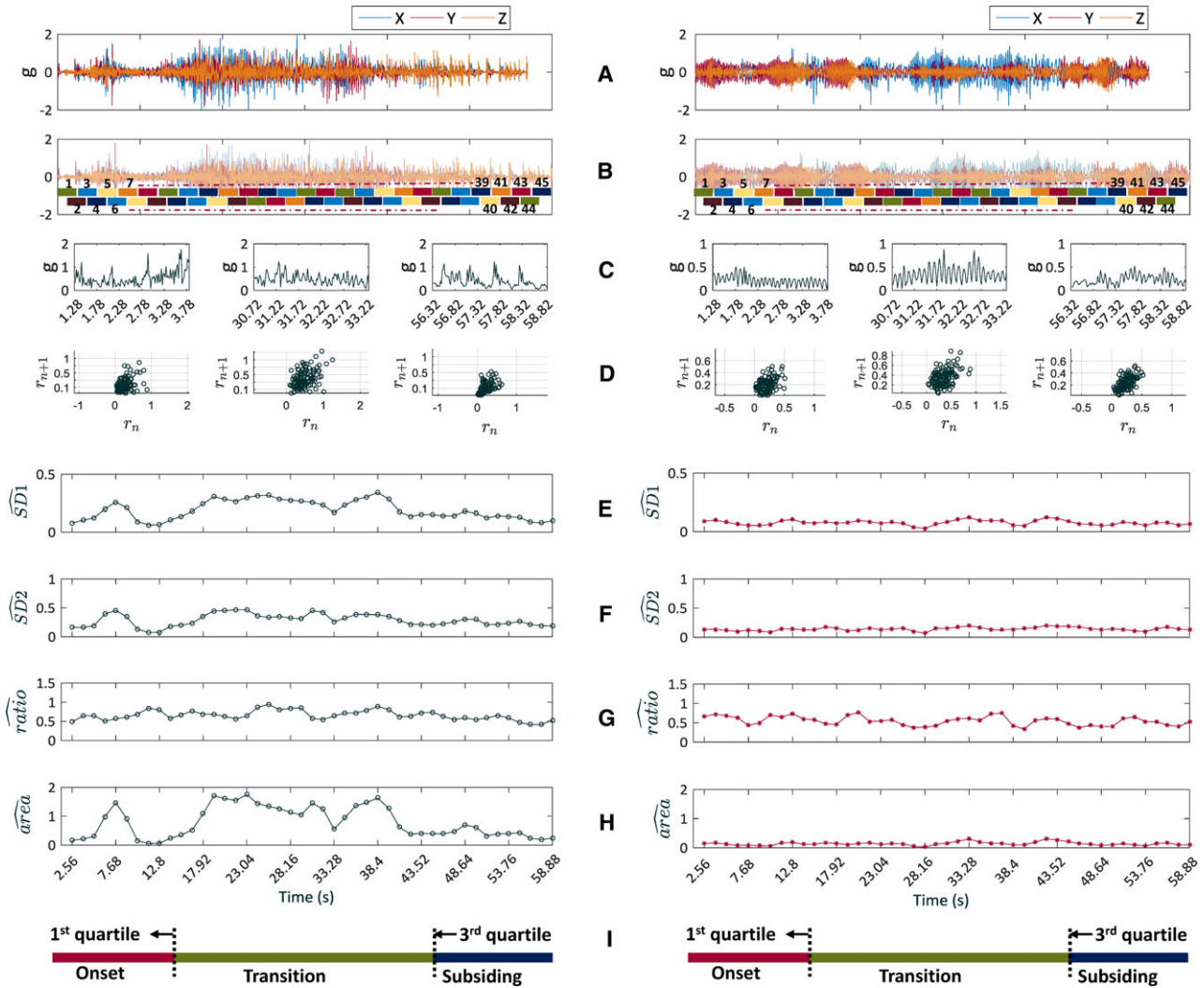


**FIGURE 1** Protocol for analysis of temporal variations: Column 1 shows a generalized tonic-clonic seizure (GTCS), and Column 2 shows a psychogenic nonepileptic seizures (PNES) event; In each column, (A) is raw signal, (B) shows the signal after resampling to 60 seconds. The resampled signal is analyzed in 2.56 second epochs with 50% overlap, and a total of 45 epochs are obtained by this windowing procedure. The epochs are shown by colored blocks of 2.56 seconds; (C) shows 2.56 second accelerometer epochs (resultant signal) during start (1.28-3.78 s), during (30.72-33.22 s), and at the end of an event (56.32-58.82 s); (D) shows the Poincaré maps corresponding to each 2.56 second epoch; (E), (F), (G), and (H) show temporal evolution of extracted Poincaré features in windows of 2.56 seconds over the course of an event, and (I) shows the division of an event into quartiles where the first quartile division (block in red) represents the temporal variations during onset, the last quartile division (block in purple) represents the subsiding behavior, and the region (block in green) between first and third quartiles represents the transition from onset to subsiding period

of an event we introduce another parameter that is termed dispersion decay index (DDI). Both of the indices are described by the following.

### 2.5.1 | Tonic index

The TI can be described as the ratio of the coefficient of variation (CoV) of the descriptors in first quartile (onset) to CoV of the descriptor over the rest of the signal.

The onset of a GTCS event involves increased muscle tone, represented by stiffening limb movements that manifest as long-term variations, resulting in high SD2 and low SD1. However, as the muscle tone decreases, high-

frequency clonic jerking begins, which involves more short-term changes, resulting in low SD2 and high SD1. Therefore, the quotient of the covariance of the computed features captures the variations during the onset relative to rest of the seizure. The TI can be explained as shown in Equation 3.

$$TI_D = \frac{CoV(\{D_{k1}\})}{CoV(\{D_{k2}\})} \quad (3)$$

where  $CoV = \left( \frac{\text{standard deviation}[SD]}{\text{mean}} \right) * 100$ , {D} represents a discrete time series for Dth descriptor (SD1, SD2, ratio, and area),  $[1 \leq k1 \leq N/4]$ ,  $[N/4 + 1 \leq k2 \leq N]$

and  $N = 45$  is the total number of 2.56 second windows (50% overlap) for an event of duration 60 seconds.

## 2.5.2 | Dispersion decay index

The DDI measures the relative change in dispersion or randomness as an event subsides. DDI captures the variance or randomness of an event in first 3 quartiles relative to the last quartile.

The high-frequency clonic jerks in a GTCS event can be characterized by an increased dispersion of the ACM traces. However, the frequency of the jerks subsides as the event progresses toward termination, which results in a lower dispersion in the last quartile. A high variance of the computed features represents increased dispersion and a chaotic motion. Therefore, the quotient of the variance of the 2 intervals captures the change in dispersion as an event subsides.

The DDI can be described as shown in Equation 4.

$$\text{DDI}_D = \frac{\text{Var}(\{D_{k1}\})}{\text{Var}(\{D_{k2}\})} \quad (4)$$

where  $\{D\}$  represents a discrete time series for  $D$ th descriptor (SD1, SD2, ratio, and area),  $[1 \leq k1 \leq 3*N/4]$ ,  $[3*N/4 + 1 \leq k2 \leq N]$  and  $N = 45$  is the total number of 2.56 second windows (50% overlap) for an event of duration 60 seconds.

## 2.6 | Statistical analysis

The statistical analysis includes the 2-sided nonparametric Mann-Whitney  $U$  test to compare the mean TI and DDI values for GTCS and convulsive PNES events. Statistical significance was considered for  $P < 0.001$ , and the area under the receiver-operating characteristic (ROC) curve (AUC) was used to evaluate the classification performance.<sup>22</sup> All statistical analysis was performed using Matlab2015b (MathWorks).

## 2.7 | Statistical machine learning: development of automated classifiers

The next step was to build an automated classifier using the new ACM features. A support vector machine (SVM)<sup>23</sup> classifier was trained using the TI and DDI of all Poincaré descriptors. We performed a leave-one-patient-out validation, where SVM was trained using data from  $N-1$  patients ( $N = 18$ ), and the learned classification model was then used to classify the events of the left-out patient. The classification performance was measured in terms of PNES detection sensitivity, specificity, positive predictive value (PPV), classification accuracy, and

Fscore. For a full description of the classification algorithm refer to Data S1.

## 2.8 | Blinded review

To validate the clinical usefulness and potential of the proposed ACM features, a blinded review was conducted by presenting the temporal evolution of the extracted Poincaré descriptors (Figure 1E-H) to 2 certified clinical neurologists (coauthors B. Yan and T.J. O'Brien). The neurologists were required to label the events as either GTCS or convulsive PNES, or term the event as nondiagnostic (the consensus decision was registered). During the whole exercise, the neurologists were blinded to the ground truth (VEM diagnosis) and all other neurophysiologic data.

## 3 | Results

### 3.1 | Seizure data collected with ACM device

Of the 79 recruited patients, 35 (44.3%) had seizures, among which 20 patients (25.3%) had convulsive seizures and 15 (18.9%) patients had nonconvulsive seizures. Of the 20 patients with convulsive seizures, 11 (55%) had GTCS events, 6 (30%) had PNES events, one had complex partial seizures (CPS), one had multiple types of seizures (GTCS+CPS), and one patient had comorbid epilepsy (PNES+GTCS). The seizure cohort comprised 60% female participants and the mean participant age was 31.6 years (20-38.2, median 29). The demographics of the seizure cohort are shown in Table S1. A total of 83 events were recorded during the monitoring period, which included 39 (46.9%) GTCS from 12 (15.2%) patients and 44 (53%) convulsive PNES events from 7 (8.8%) of 79 patients (Table S1).

### 3.2 | Motor manifestation of GTCS and convulsive PNES

A GTCS event has a clearly defined motor symptomatology as seen on VEM: tonic phase followed by a clonic phase (Figure 2); however, seizures are heterogeneous. Therefore, a clear distinction between phases may not always be possible. Nonetheless, the motor symptomatology of every GTCS event can be defined using a combination of different phases (Figure 2). The motor manifestation of a GTCS event can be characterized by an onset that involves stiffening movements due to increased muscle tone accompanied with irregular and asymmetric jerking (Figure 3A), followed by tremulousness that translates into clonic activity before subsiding gradually where the movement activity was interrupted by silent periods (shown by

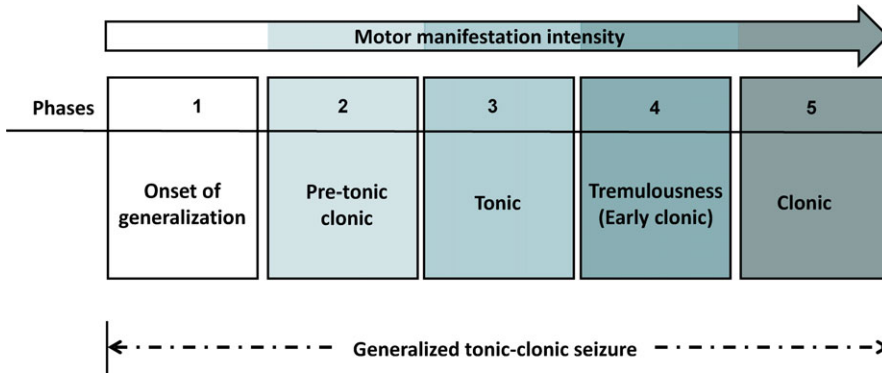


**FIGURE 2** Clinically defined phases of a generalized tonic-clonic seizure (GTCS) event with progression in the direction of the arrow; any GTCS event can be defined using a combination of these phases. The intensity of motor activity increases in the direction of the arrow; and the first 3 phases characterize the onset of a GTCS event

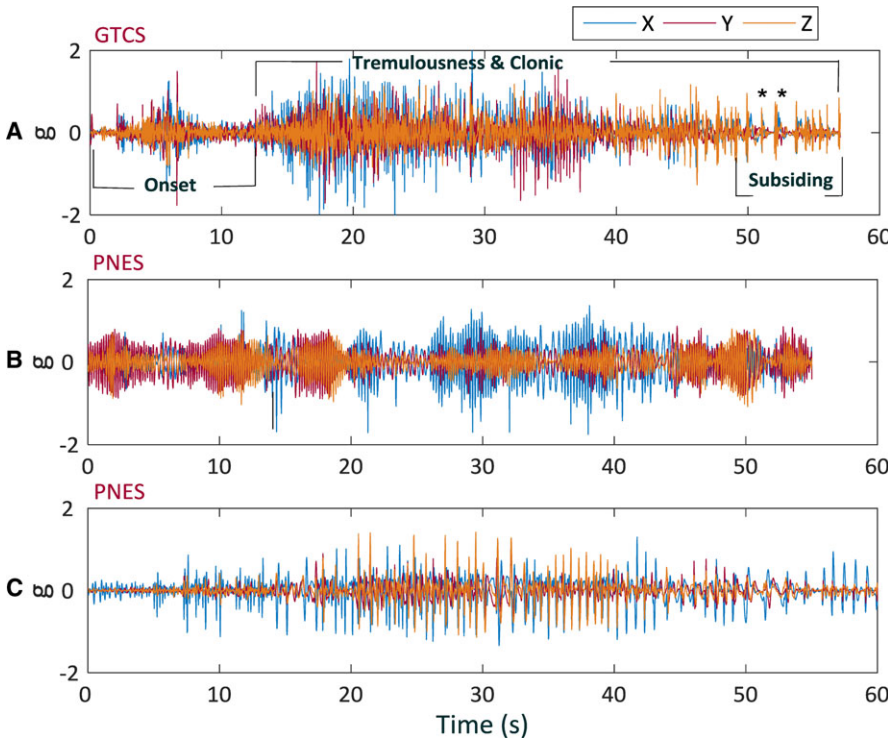


**FIGURE 3** Accelerometer (ACM) traces of typical events. A, Generalized tonic-clonic seizure event with demarcations highlighting onset, tremulousness + clonic, and subsiding behavior. The asterisk (\*) shows the silent periods as the event terminates. B, Convulsive psychogenic nonepileptic seizure (PNES) event where the tonic and the clonic phases are not separable. The envelope of the event is continuously waxing and waning over the course of an event. C, A convulsive PNES event stereotypical of a clonus activity; note the presence of multiple silent periods over the course of the event. X, Y, and Z represent the ACM traces across the 3 Cartesian coordinates

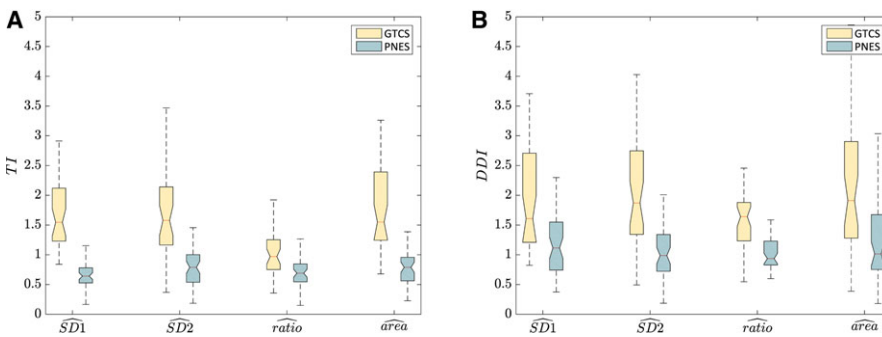


**FIGURE 4** The tonic index (TI) (A), and dispersion decay index (DDI) (B) for descriptors SD1, SD2, ratio, and area shown as box and whisker plots for generalized tonic-clonic seizure (GTCS) and convulsive psychogenic nonepileptic seizure (PNES) events

(\*) in Figure 3A). In contrast, 35 (79.5%) of 44 recorded PNES events had overlapping phases (Figure 3 B), whereas 9 events (20.5%) had a clonic phase that was separable from the tonic phase in the ACM recordings (Figure 3C). The PNES events with separable phases involved quasi-repetitive movements that had multiple silent periods over the course of the event (Figure 3C). Therefore, the motor

manifestation of GTCS and convulsive PNES shows distinct temporal dynamics.

### 3.3 | Tonic index

The TI of SD1 was significantly higher for GTCS (1.04–2.60; median 1.65) as compared to convulsive PNES (0.24–

**TABLE 1** Median, interquartile range, and area under the ROC curve (AUC) statistics for TI and DDI of Poincaré-derived descriptors corresponding to GTCS and convulsive PNES events

Index	GTCS	PNES	P value	AUC
	(median ± IQR)	(median ± IQR)		
TI <sub>SD1</sub>	1.65 ± 0.69	0.66 ± 0.22	5.48 exp(−13)	0.95
TI <sub>SD2</sub>	1.70 ± 1.16	0.80 ± 0.42	1.29 exp(−10)	0.91
TI <sub>ratio</sub>	1.05 ± 0.64	0.69 ± 0.29	7.00 exp(−06)	0.78
TI <sub>area</sub>	1.68 ± 0.99	0.81 ± 0.41	1.06 exp(−12)	0.94
DDI <sub>SD1</sub>	1.56 ± 1.48	1.05 ± 0.77	3.94 exp(−05)	0.76
DDI <sub>SD2</sub>	1.86 ± 1.26	0.94 ± 0.50	2.67 exp(−06)	0.80
DDI <sub>ratio</sub>	1.79 ± 0.70	0.92 ± 0.34	2.09 exp(−09)	0.88
DDI <sub>area</sub>	1.64 ± 1.57	0.98 ± 0.89	4.21 exp(−04)	0.72

AUC, area under the receiver-operating characteristic curve; DDI, dispersion decay index; GTCS, generalized tonic-clonic seizure; PNES, psychogenic nonepileptic seizure; TI, tonic index.

1.33; median 0.66) (Figure 4A). The TI of SD1 resulted in an AUC of 0.95 (Table 1). This shows that a good class separation can be achieved using TI of SD1. Similarly, the TI of SD2 was significantly higher for GTCS (0.83-3.64; median 1.70) in comparison to convulsive PNES (0.21-1.43; median 0.80) (Figure 4A). An AUC value of 0.91 could be achieved using TI of SD2 (Table 1). Furthermore, the TI of area was also significantly higher for GTCS (1.04-2.99; median 1.68) in comparison to convulsive PNES (0.27-1.34; median 0.81) (Figure 4A) and showed an AUC value of 0.94 (Table 1). In contrast, the TI of ratio was found to have a much lower AUC value of 0.78, while having a significant difference between GTCS (0.46-2.40; median 1.05) and convulsive PNES (0.29-1.29; median 0.69) (Figure 4A). The TI performs well for all the descriptors except ratio, and the TI of SD1 showed the best class separation between GTCS and convulsive PNES with an AUC value of 0.95 (Table 1).

**TABLE 2** The diagnostic performance of the proposed approach based on the blinded analysis of Poincaré descriptors; and an automated classifier based on the TIs and DDIs of GTCS and convulsive PNES events

Diagnosis Gold Standard	n	PNES	PNES	GTCS	GTCS	Nondiagnostic	Acc* (%)	Sens* (%)	Spec* (%)	PPV*(%)	Fscore* (%)
		TP <sup>a</sup>	FP <sup>b</sup>	TN <sup>c</sup>	FN <sup>d</sup>						
Blinded review	83	26	5	33	11	8	78.7	70.3	86.8	83.9	76.5
Automated classifier	83	42	2	37	2	N/A	95.2	95.5	94.9	95.5	95.5

<sup>a</sup>TP is the number of psychogenic nonepileptic seizure (PNES) events distinguished correctly.

<sup>b</sup>Type I error: number of false positives, that is, the number of generalized tonic-clonic seizure (GTCS) events distinguished as PNES.

<sup>c</sup>TN is the number of GTCS events distinguished correctly.

<sup>d</sup>Type II error: number of false-negatives, that is, the number of PNES events distinguished as GTCS.

\*Statistical measures of performance: overall accuracy,  $ACC(\frac{TP+TN}{TP+TN+FP+FN})$ ; Sens, sensitivity ( $\frac{TP}{TP+FN}$ ); Spec, specificity ( $\frac{TN}{TN+FP}$ ); PPV, positive predictive value ( $\frac{TP}{TP+FP}$ ); and Fscore:  $\frac{2*TP}{2*TP+FP+FN}$ . All metrics shown are calculated using the optimal threshold of the classifier except for the blinded review by epileptologists.

### 3.4 | Dispersion decay index

The DDI of SD1 was significantly different for GTCS (0.87-4.57; median 1.56) and convulsive PNES (0.46-2.57; median 1.05) (Figure 4B) events, with an AUC of 0.76. Similarly, the DDI of SD2 was significantly higher for GTCS (0.67-3.23; median 1.86) in comparison to convulsive PNES (0.41-2.90; median 0.94) (Figure 4B). However, the AUC of 0.80 for DDI of SD2 was slightly higher than the DDI of SD1 (AUC 0.76) (Table 1). Similarly, the difference in DDI of area was also statistically significant for GTCS (0.53-7.22; median 1.64) and convulsive PNES (0.33-3.22; median 0.98); however, a considerable class overlap was seen using DDI of area (AUC 0.72) (Figure 4B). In contrast, the DDI of ratio showed a better class separation (AUC 0.88) (Table 1). The DDI of ratio was significantly higher for GTCS (0.92-2.87; median 1.79) in comparison to convulsive PNES (0.64-1.53; median 0.92) (Figure 4B). Thus, it can be seen that the DDI of ratio shows the highest class separation between GTCS and convulsive PNES, which suggests that ratio is the most efficient Poincaré descriptor to capture dispersion or randomness in movement of limbs as an event subsides.

### 3.5 | Automated classifier

Using TI and DDI of all descriptors (total of 8 features as shown in Table 1), a classification model was built using SVM (refer to Data S1 for full description of the algorithm). The machine learning model correctly classified seizure-like events as PNES in 42 (sensitivity: 95.5%) of 44 PNES events and as GTCS in 37 (specificity: 94.9%) of 39 GTCS events, whereas the PPV and Fscore were both 95.5%, respectively (Table 2).

### 3.6 | Blinded review

Based on the temporal dynamics of GTCS and convulsive PNES, the following criteria were defined for

differentiating GTCS and PNES: the Poincaré-derived temporal variations (SD1, SD2, ratio, and area) in GTCS events demonstrate a continuously evolving nature (left subcolumn of Figure 1E-H). In contrast, the Poincaré-derived temporal variations in PNES events were relatively stable over the course of a convulsive PNES event (right subcolumn of Figure 1E-H). In the blinded analysis, the epileptologists correctly classified 26 of 37 events as PNES (sensitivity: 70.3%) and 33 of 38 as GTCS (specificity: 86.8%), whereas one GTCS and 7 PNES events were classified as nondiagnostic.

## 4 | DISCUSSION

Seizures have a heterogeneous manifestation and exhibit considerable intra- and interpatient variability. Given the variability across events, trained personnel with considerable experience are required for a confirmed diagnosis. In this study, we present a novel method for the differential diagnosis of convulsive PNES based on the rhythmic limb movement patterns captured using a wrist-worn ACM device. Novel ACM features to quantify the temporal variations in limb movement during seizures were proposed: (a) TI and (b) DDI.

### 4.1 | Performance of tonic index

The TI captures the mean normalized variability during the onset of an event relative to the rest of the event. The onset of a GTCS event has a defined organic pathway and can be captured using a wrist-worn ACM-based device (Figure 3). The Poincaré-derived temporal variations showed a specific evolution in time throughout the course of a GTCS event: a gradual onset that peaks during the tonic phase (left subcolumn of Figure 1E,F,H). This pattern was not observed during convulsive PNES events (right subcolumn of Figure 1E,F,H). Therefore, the TI of Poincaré-derived temporal variations for GTCS events were higher in comparison to the PNES events (Figure 4A,  $P < 0.001$ ). Among all the Poincaré-derived descriptors,  $TI_{SD1}$ ,  $TI_{SD2}$ , and  $TI_{area}$  showed a high class separation between GTCS and convulsive PNES (Table 1). The descriptors SD1, SD2, and *area* showed a continuously evolving pattern including a prominent onset for GTCS events, whereas the descriptors were comparatively stable or had less variability over the course of a convulsive PNES event (Figure 1E,F,H). Therefore, the TI of descriptors (SD1, SD2, and *area*) showed the best discriminative ability for GTCS and convulsive PNES. On the other hand, both GTCS and convulsive PNES events showed a continuously evolving pattern for *ratio* (Figure 1G); therefore, the TI of *ratio* showed the least discriminative ability.

### 4.2 | Performance of dispersion decay index

Although TI captures the temporal variations during the onset, the DDI captures the subsiding pattern of an event. DDI measures the variance in two-thirds of the signal relative to the last quartile. GTCS events involve a clonic phase that follows the tonic phase. The clonic phase can be characterized by high-frequency jerking movements of the limbs. The frequency of these clonic jerks decreases as the event terminates (the silent periods shown by (\*) in Figure 3A), leading to a lower variance in the last quartile relative to rest of the signal ( $P < 0.001$ ). However, no such pattern was observed in convulsive PNES events with distinct tonic and clonic phases. All these cases of PNES involved quasi-periodic movements; the clonus activity continued after the silent periods (Figure 3C). Therefore, DDIs of Poincaré-derived temporal variations for GTCS events were higher in comparison to PNES events (Figure 4B,  $P < 0.001$ ). Among DDIs of all the Poincaré-derived descriptors, the  $DDI_{ratio}$  showed the highest AUC for differentiating GTCS and convulsive PNES (Table 1). Ratio is a measure of randomness or dispersion in a time-varying signal; therefore, the DDI of *ratio* ( $DDI_{ratio}$ ) has the highest AUC in comparison to rest of the descriptors (Table 1 and Figure 4B).

Among TIs and DDIs, the TI of Poincaré-derived descriptors showed a higher class separation (Figure 4 and Table 1). The reason for the better performance of TI can be attributed to the more distinct onset phase in GTCS than in convulsive PNES. These findings indicate that convulsive PNES events have a characteristic nonevolving pattern on the time scale over the course of an event. By contrast, GTCS events have distinct phases and thus exhibit a continuously evolving pattern on the time scale. Given that the proposed approach is based on a timescale analysis, the validity of this approach further reinforces the findings of the preliminary study by Vinton et al.,<sup>24</sup> who showed that convulsive PNES events display a characteristic pattern of rhythmic EEG artifact with a stable nonevolving frequency footprint that differs from the evolving pattern during an epileptic seizure.

### 4.3 | Performance of automated classifier vs blinded review

The TI and DDI of Poincaré-derived temporal variations were found to be a reliable and objective marker for differentiating between GTCS and convulsive PNES, with GTCS events demonstrating significantly higher values of TI and DDI (Table 1). The automated classifier achieved a PNES detection sensitivity of 95.5% (95% confidence interval [CI] 90%-96%) and a specificity of 94.87% (95% CI 87%-

99%) (Table 2). Two PNES and 2 GTCS events were misclassified by the automated approach, resulting in diagnostic accuracy that was superior to the blinded review of Poincaré-derived temporal variations by epileptologists (Table 2). In addition, 7 of 8 events labeled as nondiagnostic during the blinded review belonged to a single patient (P<sub>17</sub>; Table S1). The automated classifier correctly differentiated all the 7 PNES events of P<sub>17</sub> that were labeled nondiagnostic (PNES cases without rhythmic clonic movements) (Table S2). Therefore, the results suggest that the new quantitative features (TI and DDI) are performing better than the qualitative assessment of features by experts. However, the blinded analysis of the Poincaré-derived temporal variations was of utmost importance, as it ensured removal of any bias that the automated classifier might have had towards the gold standard VEM diagnosis.

Furthermore, it is important to recognize that a patient can experience both types of seizures (GTCS and PNES). In a study by Jones et al<sup>1</sup> it was found that 8.1%-17.9% of the patients admitted to our VEM unit had comorbid epilepsy along with PNES. In this study, one patient experienced both seizure types (P<sub>5</sub>, Table S1) and the automated classifier was able to differentiate all GTCS and PNES events correctly, thus illustrating the importance of long-term longitudinal recordings that can capture a greater number of patient's typical seizures and present the entire diagnostic picture. This is possible by outpatient monitoring where ACM-based devices can be a feasible solution. Therefore, the new ACM features (TI and DDI) show the potential for a significant positive impact on the clinical management and prognosis of patients with PNES.

#### 4.4 | Comparison with existing studies

As a first comparison we compare the results of the proposed approach to our previously published method.<sup>15</sup> In our previous study,<sup>15</sup> we showed that a 32% cutoff on CoV of limb movement frequency differentiated between convulsive epileptic seizures and PNES. In contrast to the previous approach based on a stringent CoV threshold (AUC: 0.78), the proposed automated classifier (AUC: 0.96) resulted in better performance ( $\Delta$ AUC: 0.18,  $P = 0.002$ ). The better performance of the proposed approach can be attributed to the multiple Poincaré-derived parameters (Table 1) in comparison to a single frequency-based index proposed earlier.

Although non-EEG-based differential diagnosis of PNES is seldom discussed, a few research groups have investigated different modalities for diagnosing nonepileptic seizures.<sup>16,25</sup> Electrocardiography (ECG)-derived ictal heart rate variability (or HRV) parameters differentiated 88% of GTCS and 73% of PNES correctly.<sup>25</sup> However, heart rate changes may vary with the vigilance state of the person; therefore, ECG-

based systems are not specific.<sup>26</sup> Beniczky et al<sup>16</sup> investigated surface electromyography (sEMG) signals recorded from the deltoid muscles for differentiating GTCS and convulsive PNES. They showed that the HF/LF ratio (HF: high-frequency 64-256 Hz; LF: low-frequency 2-8 Hz) and root mean square (RMS) of the sEMG signal could differentiate all GTCS from convulsive PNES (sensitivity 100%). However, the proposed approach has several advantages over an sEMG-based system: continuous use of sEMG electrodes can be uncomfortable and the electrodes can detach.<sup>27</sup> In contrast, the proposed system is an electrode-less system, and thus is more comfortable and less encumbering to the patient. Moreover, the proposed approach is based on a time-domain analysis, which is computationally efficient and confers the opportunity for real-time analysis.<sup>28</sup>

#### 4.5 | Clinical utility of the proposed approach

Considerable experience is required for analysis of a patient's neurophysiologic and VEM data to make a definitive prognosis.<sup>29</sup> The proposed quantitative method yields a nonlinear projection of the three-dimensional (3D) rhythmic limb movement into a numerical score, thus allowing reliable distinction between GTCS and convulsive PNES with less experience. In addition, wearable ACM-based devices can be used reliably for long-term continuous monitoring of patients<sup>14</sup>; therefore, in the future, the clinical utility of the proposed approach can be further enhanced into a wearable device by the incorporation of automated algorithm for detection and differentiation of GTCS and convulsive PNES.

At this stage, an analysis of other convulsive epileptic and nonepileptic types was beyond the scope and limitations of the current study. However, it is probable that TI and DDI may also facilitate identification of other seizure types that do not manifest as rhythmic clonic activity, as in complex partial seizures.<sup>14</sup> Nonetheless, the proposed method can help overcome the limitations of the current diagnostic procedures<sup>7,29</sup>; and shows the potential to be used as a diagnostic tool to assist epileptologists in differentiating GTCS and convulsive PNES.

#### ACKNOWLEDGMENT

We declare that we have overseen and endorse the content of the manuscript being submitted for review. To date this work has not been previously submitted or is under review at another journal. Furthermore, to our knowledge, no reports have been previously submitted on identical or similar research, which has been deemed redundant. We are grateful to all the patients who agreed to be a part of the study and extend gratitude to the staff and honors students of Melbourne Brain Center for aiding in data collection.

## DISCLOSURE

None of the authors have any conflict of interest to be disclosed. We confirm that this report is consistent with the Journal's position on issues involved in ethical publication.

## REFERENCES

- Jones SG, O'Brien TJ, Adams SJ, et al. Clinical characteristics and outcome in patients with psychogenic nonepileptic seizures. *Psychosom Med*. 2010;72:487–97.
- Reuber M. Psychogenic nonepileptic seizures: answers and questions. *Epilepsy Behav*. 2008;12:622–35.
- LaFrance WC, Devinsky O. Treatment of nonepileptic seizures. *Epilepsy Behav*. 2002;3:19–23.
- Ghougassian DF, D'Souza W, Cook MJ, et al. Evaluating the utility of inpatient video-EEG monitoring. *Epilepsia*. 2004;45:928–32.
- LaFrance WC, Baker GA, Duncan R, et al. Minimum requirements for the diagnosis of psychogenic nonepileptic seizures: a staged approach. *Epilepsia*. 2013;54:2005–18.
- Smith PE. Epilepsy: mimics, borderland and chameleons. *Pract Neurol*. 2012;12:299–307.
- Devinsky O, Gazzola D, LaFrance WC. Differentiating between nonepileptic and epileptic seizures. *Nat Rev Neurol*. 2011;7:210–20.
- Reuber M, Fernandez G, Bauer J, et al. Diagnostic delay in psychogenic nonepileptic seizures. *Neurology*. 2002;58:493–5.
- Reuber M, Baker GA, Gill R, et al. Failure to recognize psychogenic nonepileptic seizures may cause death. *Neurology*. 2004;62:834–5.
- Reuber M, House AO, Pukrop R, et al. Somatization, dissociation and general psychopathology in patients with psychogenic nonepileptic seizures. *Epilepsy Res*. 2003;57:159–67.
- Alving J, Beniczky S. Diagnostic usefulness and duration of the inpatient long-term video-EEG monitoring: findings in patients extensively investigated before the monitoring. *Seizure*. 2009;18:470–3.
- Reuber M, Pukrop R, Bauer J, et al. Outcome in psychogenic nonepileptic seizures: 1 to 10-year follow-up in 164 patients. *Ann Neurol*. 2003;53:305–11.
- van Andel J, Thijs RD, de Weerd A, et al. Non-EEG based ambulatory seizure detection designed for home use: what is available and how will it influence epilepsy care? *Epilepsy Behav*. 2016;57:82–9.
- Kusmakar S, Karmakar CK, Yan B, et al. Automated detection of convulsive seizures using a wearable accelerometer device. *IEEE Trans Biomed Eng*. 2018 Jun 11 [Epub ahead of print].
- Bayly J, Carino J, Petrovski S, et al. Time-frequency mapping of the rhythmic limb movements distinguishes convulsive epileptic from psychogenic nonepileptic seizures. *Epilepsia*. 2013;54:1402–8.
- Beniczky S, Conradsen I, Moldovan M, et al. Quantitative analysis of surface electromyography during epileptic and nonepileptic convulsive seizures. *Epilepsia*. 2014;55:1128–34.
- Del Negro CA, Wilson CG, Butera RJ, et al. Periodicity, mixed-mode oscillations, and quasiperiodicity in a rhythm-generating neural network. *Biophys J*. 2002;82:206–14.
- Karmakar CK, Gubbi J, Khandoker AH. Analyzing temporal variability of standard descriptors of Poincaré plots. *J Electrocardiol*. 2010;43:719–24.
- Brennan M, Palaniswami M, Kamen P. Do existing measures of Poincaré plot geometry reflect nonlinear features of heart rate variability? *IEEE Trans Biomed Eng*. 2001;48:1342–7.
- Khandoker AH, Karmakar C, Brennan M. *Poincaré plot methods for heart rate variability analysis*. Berlin, Germany: Springer; 2013.
- Yazdi N, Ayazi F, Najafi K. Micromachined inertial sensors. *Proc IEEE*. 1998;86:1640–59.
- Hanley JA, McNeil BJ. A method of comparing the areas under receiver operating characteristic curves derived from the same cases. *Radiology*. 1983;148:839–43.
- Chang CC, Lin CJ. LIBSVM: a library for support vector machines. *ACM Trans Intell Syst Technol*. 2011;2:27.
- Vinton A, Carino J, Vogrin S, et al. Convulsive nonepileptic seizures have a characteristic pattern of rhythmic artifact distinguishing them from convulsive epileptic seizures. *Epilepsia*. 2004;45:1344–50.
- Ponnusamy A, Marques JL, Reuber M. Comparison of heart rate variability parameters during complex partial seizures and psychogenic nonepileptic seizures. *Epilepsia*. 2012;53:1314–21.
- Ramgopal S, Thome-Souza M, Jackson NE, et al. Seizure detection, seizure prediction, and closed-loop warning systems in epilepsy. *Epilepsy Behav*. 2014;37:291–307.
- Schulze-Bonhage A, Sales F, Wagner K, et al. Views of patients with epilepsy on seizure prediction devices. *Epilepsy Behav*. 2010;18:388–96.
- Logesparan L, Casson AJ, Rodriguez-Villegas E. Optimal features for online seizure detection. *Med Biol Eng Comput*. 2012;50:659–69.
- Benbadis SR, LaFrance WC Jr, Papandonatos GD, et al. Inter-rater reliability of EEG-video monitoring. *Neurology*. 2009;73:843–6.

## SUPPORTING INFORMATION

Additional supporting information may be found online in the Supporting Information section at the end of the article.

**How to cite this article:** Kusmakar S, Karmakar C, Yan B, et al. Novel features for capturing temporal variations of rhythmic limb movement to distinguish convulsive epileptic and psychogenic nonepileptic seizures. *Epilepsia*. 2019;60:165–174. <https://doi.org/10.1111/epi.14619>